Supporting Information

Quantum Dot Fluorescence Quenching Pathways with Cr(III) Complexes. Photosensitized NO Production from *trans*-Cr(cyclam)$(ONO)_2^+$

Daniel Neuman, Alexis D. Ostrowski, Alexander A. Mikhailovsky, Ryan O. Absalonson, Geoffrey F. Strouse and Peter C. Ford.*

List of Figures

Figure S1. Optical properties of CdSe cores in hexanes solution following purification. (solid line is the absorption spectrum; dashed line is the emission spectrum (450 nm excitation)

Figure S2. Stern-Volmer type plot showing the negligible effect of different KCl concentrations on the photoluminescence intensity at 570 nm of aqueous solutions of QDs. Each point represents an individual sample of QDs diluted to 300 nM in 15 mM phosphate buffer solution with varied concentrations of KCl added.

Figure S3. Optical data for phosphate buffered solutions of QDs (190 nM) mixed with varied concentrations of **2** (0-1000 μM).

Figure S4. Steady-State PL spectra of ~130 nM QDs in buffer (filled circles) and 130 nM QDs plus ~1 mM Cr(cyclam)$(ONO)_2^+$ (open squares) in buffer.

Figure S5. Stern-Volmer plot for solutions of QDs in phosphate buffer (15 mM, pH 8.2) at constant concentration (~190 nM) with varied concentrations of Cr(III) complex.

Figure S6. Comparison of QD PL intensity in mixtures with various Cr(cyclam)X_2^+ (500 μM)

Table S1. Time resolved PL parameters for decay of QD PL with and without added quencher, as indicated.

Table S2. Fitting parameters for double exponential fits of the QD 1S bleach decay in the presence of varied concentrations of **1**.

Other Information Provided:

Discussions of Förster Approximation for Energy Transfer and of the estimate of possible packing of Cr(III) complexes on QD surface.

Procedures used to prepare water-soluble core/shell CdSe/ZnS quantum dots.

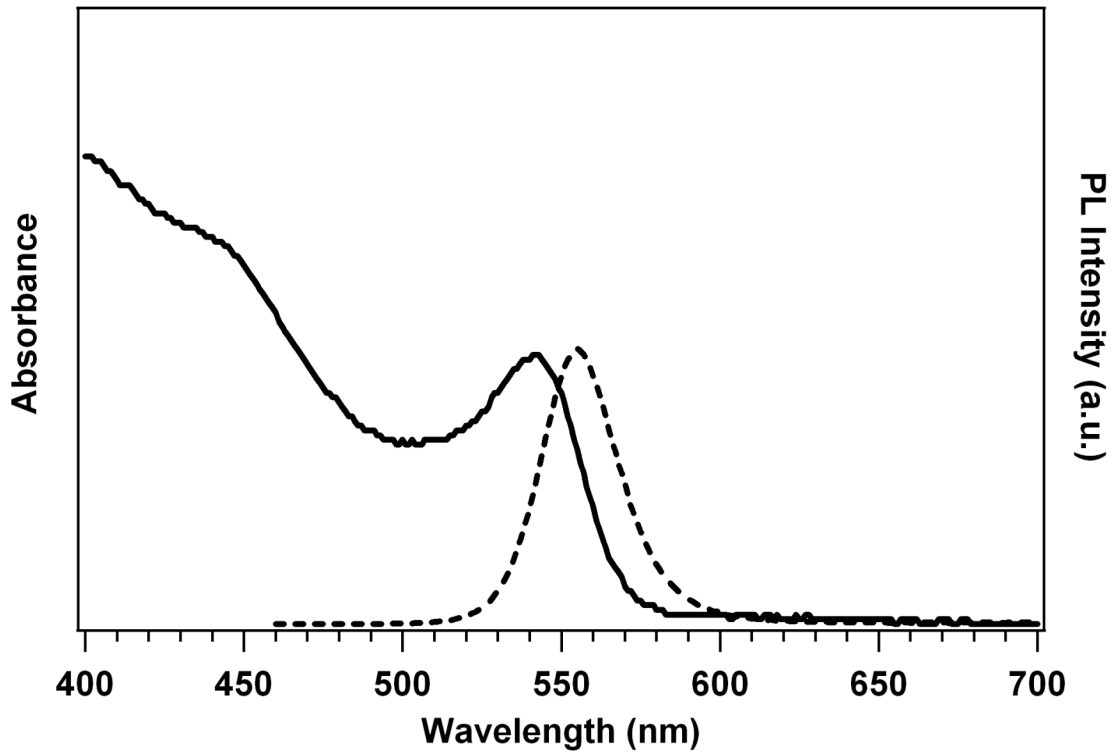

Figure S1. Optical properties of CdSe cores in hexanes solution following purification. (solid line is the absorption spectrum; dashed line is the emission spectrum (450 nm excitation)

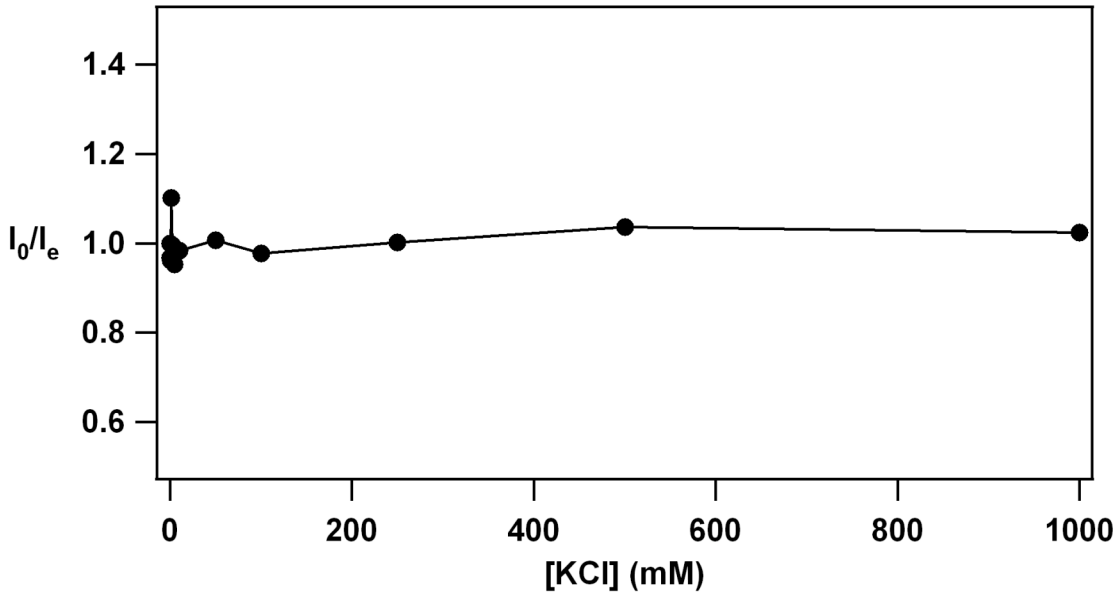

Figure S2. Stern-Volmer type plot showing the negligible effect of different KCl concentrations on the photoluminescence intensity at 570 nm of aqueous solutions of QDs. Each point represents an individual sample of QDs diluted to 300 nM in 15 mM phosphate buffer solution with varied concentrations of KCl added.

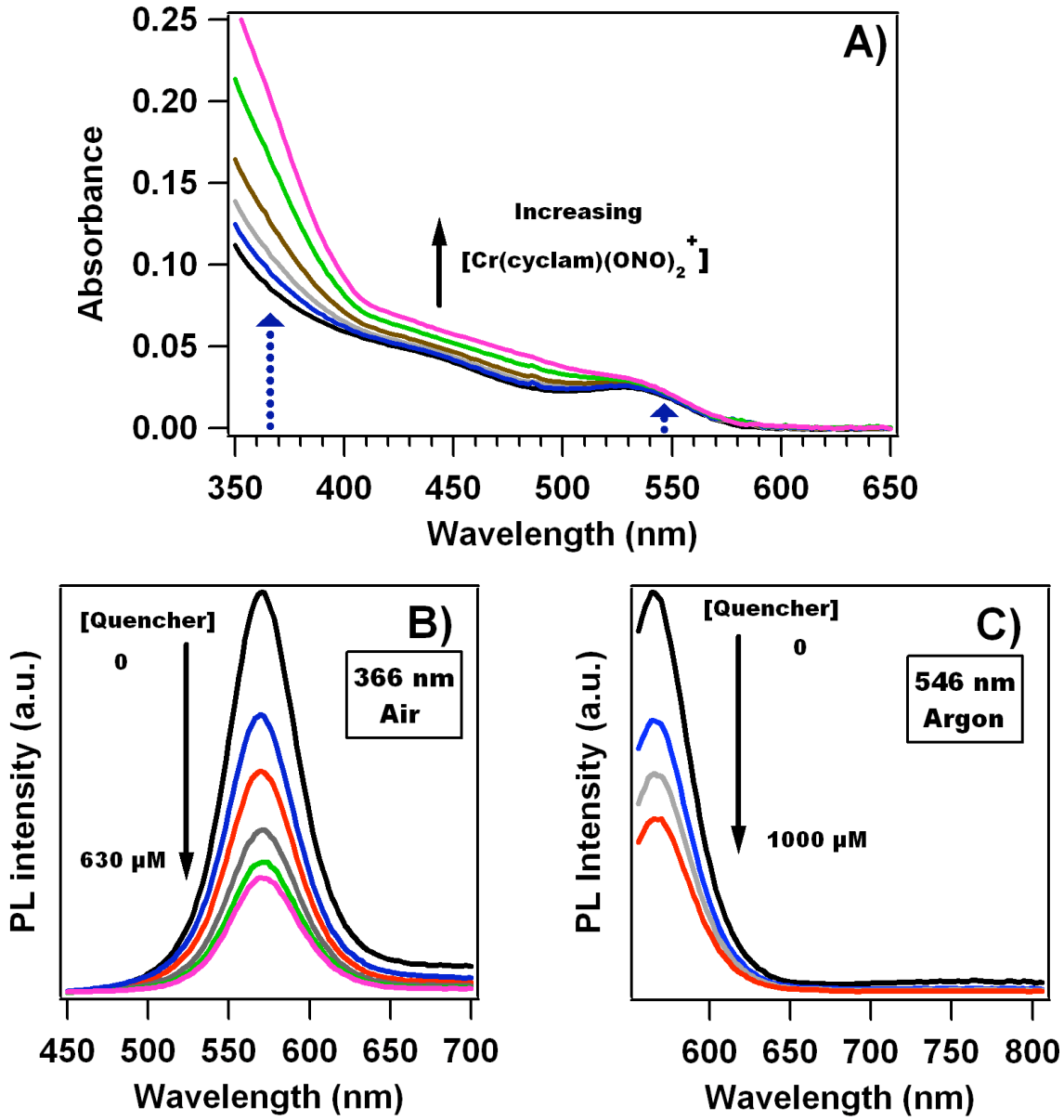

Figure S3. Optical data for phosphate buffered solutions of QDs (190 nM) mixed with varied concentrations of **2** (0-1000 µM). A) Absorbance data for mixtures of QDs (190 nM) and **2** (0-630 µM). Dotted arrows indicate 366 nm and 546 nm excitation used in B) and C), respectively. B) PL spectra of QDs (190 nM) and mixed with varied concentrations of **2** (0-630 µM) obtained with 366 nm excitation. Spectra have been corrected for inner-filter effects due to absorbance of **2** at this wavelength. C) PL spectra of QDs (190 nM) and mixed with varied concentrations of **2** (0-1000 µM) obtained with 546 nm excitation.

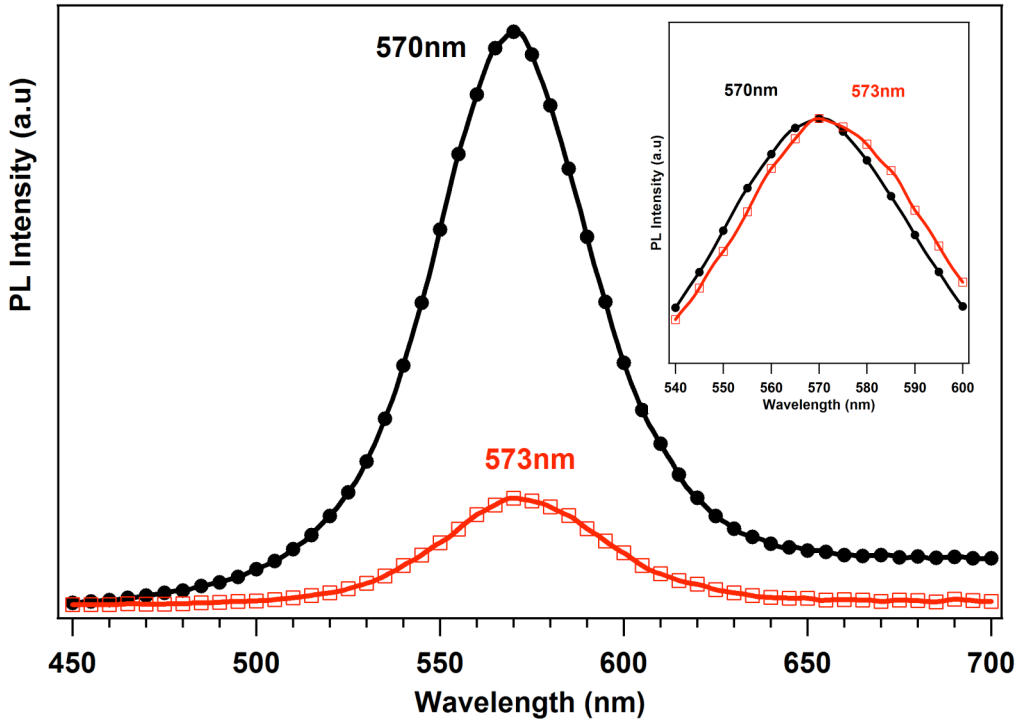

.

Figure S4. Steady-State PL spectra of ~130 nM QDs in buffer (filled circles) and 130 nM QDs plus ~1 mM $Cr(cyclam)(ONO)_2^+$ (open squares) in buffer. The peak shifts ~3 nm after the $Cr(cyclam)(ONO)_2^+$ is added. Inset shows a magnification of the normalized peaks. To resolve the peak maxima and confirm the shift upon quenching, the instrument was optimized to a resolution of 1 nm and peak maxima were determined by a Gaussian curve fitting procedure.

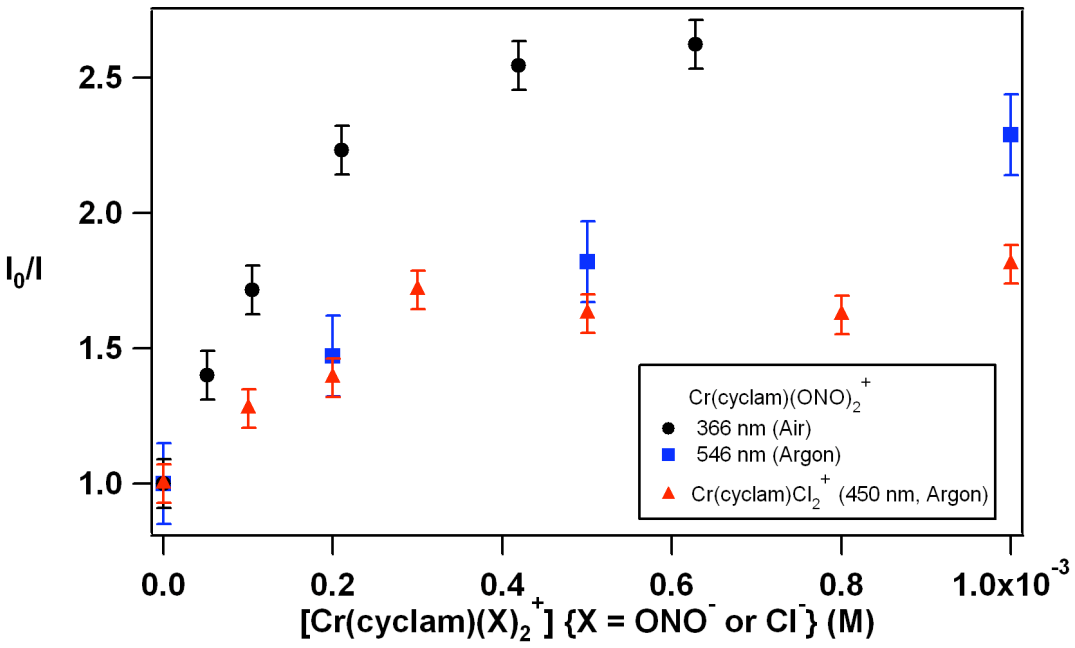

Figure S5. Stern-Volmer plot for solutions of QDs in phosphate buffer (15 mM, pH 8.2) at constant concentration (~190 nM) with varied concentrations of Cr(III) complex. I is the PL intensity at the λ_{max} and I_0 is the corresponding PL intensity of QDs without any complex added.

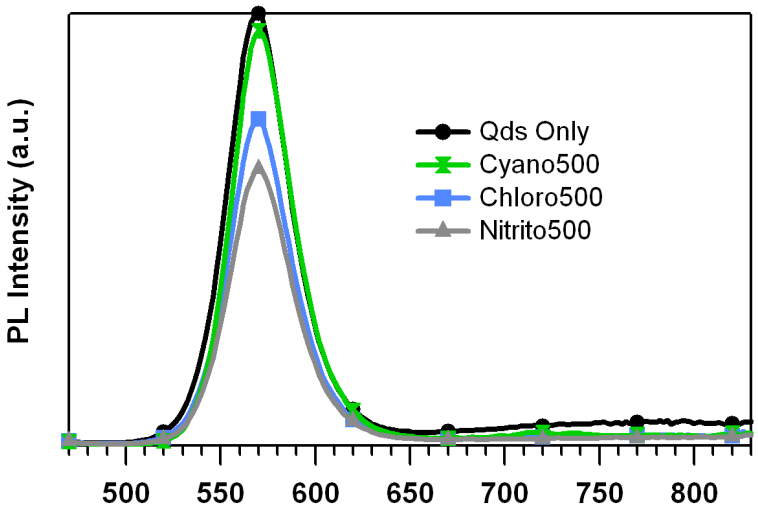

Figure S6. Comparison of QD PL intensity in mixtures with various Cr(cyclam)X_2^+ (500 μM) where X = CN^- - hourglasses; Cl^- - squares; ONO^- - triangles; QDs with no quencher - circles. All samples are diluted in phosphate buffer (15 mM, pH 8.2), contain 210 nM QDs and were sparged with argon prior to the measurements. An excitation wavelength of 460 nm is used and the PL intensities are corrected for any inner filter effects due to absorption of the added quencher. {It should be noted that these experiments were conducted with a different batch of QDs having similar spectral properties, but with a slightly lower PL quantum yield (~1 %)}.

Table S1. Time resolved PL parameters for decay of QD PL with and without added quencher, as indicated. All samples contained the same concentration of QD (210 nM) diluted in phosphate buffer and were sparged with argon prior to the measurement. The PL was excited with the 460 nm output of a frequency doubled Ti:sapphire laser (~120 fs pulses). τ in ns. {It should be noted that these experiments were conducted with a different batch of QDs having similar spectral properties, but with a slightly lower PL quantum yield (~1 %). This is clearly manifested in a higher contribution of the "ultra-fast" PL component, at the expense of the longer components. However, the changes in the fitting parameters following addition of either quencher is in analogy to that seen with samples described earlier (see for example Table 1 in the text).}

Complex (500μM)	α_1	τ_1	α_2	τ_2	α_3	τ_3	α_4	τ_4	$\Sigma\alpha_x\tau_x$
none	0.48	0.055	0.25	0.634	0.18	3.97	0.08	16.2	2.18
1	0.42	0.055	0.26	0.55	0.19	3.07	0.08	12.4	1.74
2	0.48	0.055	0.28	0.507	0.15	2.68	0.07	9.5	1.24

Table S2. Fitting parameters for double exponential fits of the QD 1S bleach decay in the presence of varied concentrations of **1**. QD concentration in each solution was 1.9 μM. τ in ps.

1 in mM	τ_1	α_1(%)	τ_2	α_2(%)
0	26	15	1900	85
5	28	26	1100	74
10	17	34	710	66

Förster Approximation for Energy Transfer.

Derivation of equations used to determine Förster overlap intergral, $J(\lambda)$, Förster radius, R_o, and the Donor (D) – Acceptor (A) separation distance, r, based on R_0 and the observed donor quenching efficiency.[1,2]
The rate of energy transfer between a single donor and single acceptor molecule is given by:

Eq. 1. $$k_{EN}(r) = \frac{Q_D \kappa^2}{\tau_{D(0)} r^6}\left(\frac{9000(\ln 10)}{128\pi^5 N n^4}\right)\int_0^\infty F_D(\lambda)\varepsilon_A(\lambda)\lambda^4 d\lambda = \frac{1}{\tau_{D(0)}}\left(\frac{R_0}{r}\right)^6 ;$$

where Q_D is the donor quantum yield in the absence of acceptor; $\tau_{D(0)}$ is the donor lifetime in the absence of acceptor; κ is the dipole-dipole orientation factor where for randomly oriented dipoles κ^2=2/3; N is Avogadro's number; n is the refractive index of the medium.

The J-overlap integral (function to the right of the integrand in Eq. 1), represented by:

Eq. 2. $$J(\lambda) = \int_0^\infty F_D(\lambda)\varepsilon_A(\lambda)\lambda^4 d\lambda .$$

represents the spectral overlap of the donor and acceptor electronic spectra. $F_D(\lambda)$ represents the integrated photoluminescence of the donor with area under the curve normalized to unity; ε_A is the wavelength dependent extinction coefficient of the acceptor. It is common to measure distances between donor and acceptor as an indicator of energy transfer efficiency and thus use of the Förster radius which is defined as:

Eq. 3. $$R_0 = \left(\frac{9000(\ln 10)\kappa^2 Q_D}{128\pi^5 N n^4}\int_0^\infty F_D(\lambda)\varepsilon_A(\lambda)\lambda^4 d\lambda\right)^{1/6}$$

and represents the donor – acceptor separation distance at which the rate of energy transfer is exactly equal to the rate of excited state decay of the donor.

Using the spectral data shown in Figure 1 of the main text, one obtains $J(\lambda) = 1.47 \times 10^{-13}$ cm^6 for the spectral overlap of the core-shell QDs used here with **1**. With a quantum yield of 0.02 for the QD PL quantum yield (Q_D), we obtain a value of R_0 = 2.8 nm for the Förster radius.

As discussed in the text, this value of R_0 along with $\tau_{D(0)}$ = 15.4 ns, can be used to calculate k_{EN} for various distances r between the QD and a single molecule of **1**.

Estimation of the Maximum # of *trans*-Cr(cyclam)Cl_2^+ Cations Packed Around a QD.

The number of acceptors around a single QD can be estimated based on steric considerations and hard-sphere packing model[3,4] according to the following equation:

Eq. 4. $$N_{Complex} = 0.65\left(\frac{\left(R_2^3 - R_1^3\right)}{R_c^3}\right)$$

where R_1 is the radius of the QD excluding the organic capping layer; $R_2 \sim R_1 + 2R_c$ is the radius of the QD plus the surrounding complex. We obtain the following values for R_1, R_2, R_c, and $N_{Complex}$.

$R_1 = R_{core} + ZnS_{thickness} = 3.8$ nm

$R_c = 0.90$ nm*

*Half of longest C to C distance in a single $Cr(cyclam)Cl_2^+$ complex estimated from crystallographic data.

$R_2 = 5.6$ nm

$N_{complex} \sim 110$.

Procedure used to prepare core/shell quantum dots:

A three step procedure involving growth of the CdSe cores, then growth of the ZnS shells around the cores, followed by surface ligand exchange with DHLA was used for the synthesis of water soluble core/shell QDs.

The CdSe cores were prepared by the decomposition of dimethylcadmium (Me_2Cd) and trioctylphosphine selenide (TOP-Se) precursors in a 40:20:40 (mol %) melt of hexadecylamine (HDA), trioctylphosphine (TOP), and trioctylphosphine oxide (TOPO) ligands according to published procedures.[5] First, TOPO (9.01 g, 23.3 mmol) was heated at 180 °C under reduced pressure for 2 h in a 50 mL, 3 neck round bottom flask. After cooling to ~60 °C under an argon flow, HDA (5.63 g, 23.3 mmol) was added and the resulting mixture was heated at 120 °C under reduced pressure for 1 h more to remove traces of O_2/H_2O. The argon flow was again started and the ligand mixture heated slowly to 330 °C, at which point, the heating mantle was removed. When the temperature cooled to 300 °C, a solution of Me_2Cd (0.172 g, 1.2 mmol) and TOP-Se (3 mL, 2.0 M) in TOP (2 mL, 4.5 mmol) was quickly injected from a gas-tight syringe with high speed stirring. Once the temperature stabilized (~150 °C), the heating mantle was returned and the temperature of the vigorously stirred mixture was raised to ~225 °C. The reaction was monitored as the QDs grew by periodically removing a small aliquot (~100 μL) and following changes in the absorbance spectrum. When the desired spectrum was obtained (~25 min), the mixture was cooled to ~60 °C and the CdSe cores were flocculated by addition of 2 volume equivalents of methanol. Following centrifugation and removal of the supernatant, the CdSe cores were dissolved in minimal hexanes (~20 mL) and centrifuged to remove insoluble by-products of the reaction. After re-flocculating with methanol, the CdSe cores were washed with another equivalent of methanol and then dried under reduced pressure. The purified QDs were then dissolved in a solution of ~0.1 M HDA in hexanes, and their size and concentration were estimated from the peak position and intensity of the lowest exciton transition correlated with the reported QD sizing curve[6] and the size dependent extinction coefficient[7] of this transition. This preparation gave ~2.4 μmol of CdSe cores with a lowest excitonic transition ($1S\text{-}1S_{3/2}$) centered at 541 nm and a narrow photoluminescence (PL) (full width at half maximum (FWHM) = 29 nm) centered at 555 nm (Figure S1) Based on the position of the $1S\text{-}1S_{3/2}$ excitonic transition, these CdSe core quantum dots have diameters of ~3.8 nm.[6] The photoluminescence quantum yield for these QDs was determined to be 11%

A zinc sulfide (ZnS) shell was grown on the CdSe cores using established procedures,[8] and amounts of precursors necessary to obtain six monolayer shells calculated from the volume ratio of a spherical shell and a spherical core using the bulk lattice parameters of CdSe and ZnS. TOPO (12.5 g, 32.3 mmol) was heated at 190 °C under reduced pressure for 2 h. After cooling to 60 °C, TOP (1.22 mL, 2.7 mmol) and the CdSe cores in hexanes (0.12 mM in 5 mL solvent) were added under argon flow. The mixture was heated at 100 °C under reduced pressure for 1 h to remove volatiles and residual O_2/H_2O and then returned to argon flow and heated to 170 °C. When the temperature stabilized, a solution of diethyl zinc (355 μL, 3.5 mmol) and hexamethyldisilathiane (730 μL, 3.5 mmol) in TOP (7 mL, 15.7 mmol) was added drop-wise from a gas tight syringe under vigorous stirring over the course of ~10 min using a syringe pump. Once the injection was complete, the temperature was lowered to ~90 °C and the core/shell QDs were allowed to anneal for 2 h. The temperature was then lowered to 70 °C and 10 mL of argon sparged n-butanol was added to prevent solidification of the TOPO upon cooling. The resulting core/shell QDs were stored in the dark in their growth mixture. Isolation/purification was affected by flocculation of the QDs with four volume equivalents of methanol. Following removal of the colorless supernatant, the QDs were washed (2x) with methanol and dried under reduced pressure. This synthesis gives core/shell QDs with a photoluminescence band centered at 561 nm (FWHM = 45 nm) and a quantum yield of ~15%.

The initial HDA/TOP/TOPO capping groups were exchanged for dihydrolipoic acid (DHLA) (freshly prepared by the reduction of lipoic acid with sodium borohydride[9a]) according to published procedures with slight modifications.[9,10] The DHLA (20 mg, 96 μmoles) was dissolved in methanol (15 mL), the pH was adjusted to ~12 with tetramethylammonium hydroxide, and the solution was entrained with Ar to remove O_2. Dried QDs (10 mg, 16 nmol) were then added under subdued light to form a suspension, and the mixture was stirred at reflux overnight under inert atmosphere. During this time the mixture became homogeneous, indicating that the DHLA thiol-groups have displaced the original hydrophobic capping ligand. After cooling to room temperature, the QDs were flocculated by adding four volume equivalents of diethyl ether and centrifuged. The QDs were re-dissolved in minimal methanol and flocculated once more with diethyl ether and centrifuged. After drying under reduced pressure, the QDs were dissolved in phosphate buffer solution (15 mM, pH 8.2) and purified using 3 cycles of concentration/dilution (10:1) with phosphate buffer in a centrifugal filtration device (Millipore, M_W cutoff ~10,000 Daltons) to give a final stock solution, aliquots of which were used for the experiments reported here. Following purification, the DHLA capped core/shell QDs had a PL maximum centered at 570 nm (FWHM = 45 nm) and a PL quantum yield of ~2 % in phosphate buffer solution (15 mM, pH 8.2). The water soluble QDs optical properties, e.g. narrow PL linewidths and quantum yields are comparable to those observed for similarly prepared QDs in aqueous solution.[4]

References.

1) Lakowicz, J. R. *Principles of Fluorescence Spectroscopy, 2nd Ed.*, Kluwer Academic, New York, **1999**.

2) Clapp, A. R. Medintz, I. L.; Mauro, J. M.; Fisher, B. R.; Bawendi, M. G.; Mattoussi, H. *J. Am. Chem. Soc.*, **2004**, *126*, 301-310.

3) Cebula, J.; Ottewill, R. H.; Ralston, J.; Pusey, P. N. *J. Chem. Soc., Faraday Trans.*, **1981**, *I77*, 2585-2612

4) (a) Mattoussi, H.; Mauro, J. M.; Goldman, E. R.; Anderson, G. P.; Sundar, V. C.; Mikulec, F. V.; Bawendi, M. G. *J. Am. Chem. Soc.*, **2000**, *122*, 12142-12150. (b) Pompa, P. P.; Chiuri, R.; Manna, L.; Pellegrino, T.; del Mercato, L. L.; Parak, W. J.; Calabi, F.; Cingolani, R.; Rinaldi, R. *Chem. Phys. Lett.* **2006**, *417*, 351-357.

5) (a) Murray, C. B.; Norris, D. J.; Bawendi, M. G. *J. Am. Chem. Soc.* **1993**, *115*, 8706-8715. (b) Talapin, D. V.; Rogach, a. L.; Kornowski, A.; Haase, M.; Weller, H. *Nano Lett.* **2001**, *1*, 207-211. (c) de Mello Donega, C.; Hickey, S. G.; Wuister, S.; Vanmaekelbergh, D.; Meijerink, A. *J. Phys. Chem. B* **2003**, *107*, 489-496.

6) Mikulec, F. V.; Kuno, M.; Bennati, M.; Hall, D. A.; Griffin, R. G.; Bawendi, M. G. *J. Am. Chem. Soc.* **2000**, *122*, 2532-2540.

7) Yu, W. W.; Qu, L.; Guo, W.; Peng, X. *Chem. Mater.* **2003**, *15*, 2854-2860.

8) Dabbousi, B. O.; Rodriguez-Viejo, J.; Mikulec, F. V.; Heine, J. R.; Mattoussi, H.; Ober, R.; Jensen, K. F.; Bawendi, M. G. *J. Phys. Chem. B* **1997**, *101*, 9463-9475.

9) (a) Uyeda, H. T.; Medintz, I. L.; Jaiswai, J. K.; Simon, S. M.; Mattoussi, H. *J. Am. Chem. Soc.*, **2005** *127*, 3870-3878. (b) Gunsalus, I. C.; Barton, L. S.; Gruber, W. *J. Am. Chem. Soc.* **1956**, *78*, 1763 – 1766. (c) Wagner, A. F.; Walton, E.; Boxer, G. E.; Pruss, M. P.; Holly, F. W.; Folkers, K. *J. Am. Chem. Soc.* **1956**, *78*, 5079 – 5081.

10) Cheng, C.-T.; Chen, C.-Y.; Lai, C.- W.; Liu, W.- H.; Pu, S.- C.; Chou, P.- T.; Chou, Y.- H.; Chiu, H.-T. *J. Mater. Chem.* **2005**, *15*, 3409 – 3414.